JOURNAL OF GEOPHYSICAL RESEARCH, VOL. 91, NO. A7, PAGES 8025–8033, JULY 1, 1986

A Laboratory Study of Ion Energization by EIC Waves and Subsequent Upstreaming Along Diverging Magnetic Field Lines

S. L. CARTIER, N. D'ANGELO, AND R. L. MERLINO

Department of Physics and Astronomy, The University of Iowa, Iowa City

A laboratory study related to energetic upstreaming ions in the ionosphere-magnetosphere system is described. The experiment was carried out in a cesium Q machine plasma with a region of nonuniform magnetic field. Electrostatic ion cyclotron waves were excited by drawing an electron current to a small biased exciter electrode. In the presence of the instability, ions are heated in the direction perpendicular to **B**. Using a gridded retarding potential ion energy analyzer, we followed the evolution of the ion velocity distribution as the ions passed through the heating region and subsequently flowed out along the diverging **B** field lines. As expected, the heated ions transfer their energy from perpendicular to parallel motion as they move through the region of diverging **B** field. Both their parallel thermal energy and the parallel drift energy increase at the expense of the perpendicular energy.

1. INTRODUCTION

The possibility that electrostatic ion cyclotron (EIC) waves which are generated on auroral field lines might be responsible for the production of energetic (keV) ion conics in the ionospheric-magnetospheric plasma has been investigated for several years. (See, for example, the review paper by *Horwitz* [1982].) The present paper describes a laboratory study of this phenomenon. We begin with a summary of previous relevant work in the earth's ionosphere-magnetosphere (section 1.1) and the laboratory (section 1.2). Also, whenever appropriate, related theoretical work is considered.

1.1. *Ionosphere-Magnetosphere*

Observations in the distant magnetotail by *Frank et al.* [1977] indicated a strong source of oxygen ions originating near the earth. *Shelley et al.* [1976], *Sharp et al.* [1977], and *Ghielmetti et al.* [1978] reported the observation, at high latitudes and at altitudes of $\sim 1\ R_E$, of two kinds of energetic ion distributions: "conics," with peak fluxes between the directions perpendicular and parallel to the magnetic field, and highly collimated distributions with peak fluxes along the magnetic field. Both distributions have net fluxes out of the ionosphere. While the latter ("ion beams") have been associated with parallel electric fields [*Croley et al.*, 1978], the "conics" are usually attributed to perpendicular ion heating at low altitudes and subsequent magnetic focusing as the energized ions move up the field lines.

The suggestion that ionospheric ions might, in fact, be accelerated by some kind of VLF waves had been made by *Klumpar* [1975]. *Kintner et al.* [1978] reported the observation of electrostatic hydrogen cyclotron waves in the polar magnetosphere at altitudes of $\sim 1\ R_E$. The electric field detector on board the S3-3 satellite often detected peaks at frequencies slightly above the first few harmonics of the H^+ cyclotron frequency. Density perturbations were also detected, suggesting that the waves were electrostatic. In addition, the presence of the waves correlated with field-aligned currents, which were known to drive EIC waves unstable. In a subsequent paper, *Kintner et al.* [1979] reported the simultaneous observation of energetic (keV) upstreaming ions and electrostatic hydrogen cyclotron waves, although the source of free energy for the EIC waves could not be determined unambiguously.

Klumpar [1979] argued that a part of the high-latitude cold ionospheric ion distribution is, at times, transversely accelerated within a "source region" as low as 1000 km. Subsequent to their transverse acceleration the ions are driven upward into the magnetosphere by the gradient B mirror force, $f = -\mu \cdot \nabla B$, where μ is the ion magnetic moment. *Ungstrup et al.* [1979] attributed the transverse ion acceleration and heating to EIC waves. Energetic ions would reach the spacecraft above the heating region, their pitch angle distribution being determined by the position of the spacecraft relative to the heating region and by the vertical extent of the heating region itself.

Recent theoretical work on EIC waves and ion acceleration in the ionosphere-magnetosphere can be found, e.g., in papers by *Okuda and Ashour-Abdalla* [1983], *Bergmann* [1984], and *Okuda and Nishikawa* [1984].

Finally, it should be added that ion heating in terms of ion interaction with EIC waves and subsequent adiabatic motion is not the only mechanism proposed to explain the formation of ion conics. For example, *Lennartsson* [1980], *Borovsky* [1981, 1984], and *Borovsky and Joyce* [1983] have argued that the same result can be accomplished by oblique double layers in strongly magnetized plasmas. Also, *Chang and Coppi* [1981] proposed a mechanism for transverse ion energization by lower hybrid waves. These waves, if of sufficient amplitude ($E_{rms} \simeq 50$ mV/m), would produce low-altitude "conics." Parallel ion energization by quasi-static electric fields, in addition, would generate nearly field aligned ion beams, which, in turn, might also excite the EIC waves observed at higher altitudes.

1.2. *The Laboratory*

Electrostatic ion cyclotron waves were observed for the first time over 2 decades ago in a Q machine by drawing an electron current along the axis of a magnetized plasma column to a small positively biased disk [*D'Angelo and Motley*, 1962; *Motley and D'Angelo*, 1963]. Waves with a frequency 10–15% larger than the ion cyclotron frequency were excited when the electron drift velocity exceeded a critical value of about 10 times the ion thermal velocity. The observations were inter-

Paper number 5A8271.
0148-0227/86/005A-8271$05.00

preted as waves propagating nearly normal to the magnetic field and radially outward from the current channel with a perpendicular wavelength, $\lambda_\perp$, such that $(2\pi/\lambda_\perp)\rho_i \approx 1$, ρ_i being the ion gyroradius.

The properties of these waves and the conditions of excitation of the instability were accounted for by *Drummond and Rosenbluth* [1962], who developed a theory appropriate to the case where the plasma is infinite, homogeneous, collisionless, and magnetized, with a uniform electron drift along the **B** field.

A few years later, *Levine and Kuckes* [1966] pointed out certain discrepancies between the Drummond and Rosenbluth theory and their own experiments. In particular, they observed that the critical electron drift velocity increased with an increasing T_e/T_i ratio, in contradiction to the predictions of the collisionless theory. However, a collisional kinetic theory of the instability had been developed by *Varma and Bhadra* [1964], who predicted a dependence of the critical drift on the T_e/T_i ratio as found by Levine and Kuckes when ion-ion collisions are taken into account.

After the work of *Levine and Kuckes* [1966], numerous laboratory investigations of the electrostatic ion cyclotron instability were conducted by various groups, notably at the University of California (UC) at Irvine [e.g., *Correll et al.*, 1975, 1977; *Dakin et al.*, 1976; *Stern et al.*, 1976; *Schrittwieser et al.*, 1984*a*, *b*], at Tohoku University, Sendai [e.g., *Hatakeyama et al.*, 1977; *Sato and Hatakeyama*, 1985], at Princeton [*Chu et al.*, 1973], at Risø [*Michelsen et al.*, 1976], at Durban [*Alport et al.*, 1983], and at Iowa [*Cartier et al.*, 1985*a*, *b*].

Particularly relevant to this report are the results on ion heating by ion cyclotron waves obtained first by the group at UC Irvine and, later, at Tohoku University. They demonstrated that large amplitude ($\delta n/n \simeq$ 20–30%) EIC waves can heat the ions in the direction perpendicular to the magnetic field by a factor as large as 10 over the normal Q machine ion temperature of 0.2–0.3 eV. This heating is predicted by numerous theories, as already stated in section 1.1. Also, *Stern et al.* [1981] have shown that the "heating" really consists of an ion ring distribution plus a background heating; i.e., although there is some heating by thermalization, much of the apparent broadening of the ion velocity distribution was due to the ion ring current, which can only be detected with the resolution available with the optical diagnostic (laser-induced fluorescence) utilized by the UC Irvine group. Further measurements were made [*Lang and Boehmer*, 1983] of parallel electric fields associated with EIC waves, which were interpreted in terms of electron trapping by the large amplitude waves.

Related to most of the laboratory experiments discussed here are the nonlocal theories of the EIC instability [e.g., *Ganguli and Bakshi*, 1982; *Bakshi et al.*, 1983], in which effects such as the finite width of the current channel are accounted for. The importance of these nonlocal effects in magnetospheric plasmas has also been discussed [*Ganguli et al.*, 1984]. These theories predict that if the width of the current channel is reduced to a few ion gyroradii, the instability is completely quenched. We have reported recently [*Cartier et al.*, 1985*b*] on a systematic test of this "filamental quenching."

In the present paper we present the results of an experiment, performed in the Iowa Q machine, in which Cs^+ ions are heated by EIC waves to values of the perpendicular temperature, $T_{i,\perp}$, as large as $\sim$1.6–1.8 eV. A transfer of energy from the perpendicular to the parallel (to **B**) ion motion, as expected from basic physics, is observed as the ions pass through the end portion of the Q device, where the magnetic field strength decreases to values as low as approximately one tenth of that in the heating region. A similar effect, for unheated ions, has been reported previously by *Hatakeyama et al.* [1974]. The behavior of EIC wave-heated ions in a diverging magnetic field is a novel feature of the present experiment.

The paper is organized as follows. Section 2 presents the minimal theoretical background needed for the interpretation of our results. Section 3 describes the experimental setup, and section 4 the experimental results and comparisons with theory. Section 5 contains a discussion of the results and the conclusions.

2. THEORETICAL BACKGROUND

This section is intended to provide a minimum theoretical background, needed for a better understanding of the experimental results to be presented in section 4. We consider here the following points: the perpendicular (to **B**) ion energization by EIC waves (section 2.1) and the evolution of the energized ion energy distribution under conditions of diverging magnetic field (section 2.2).

2.1. *Ion Energization by EIC Waves*

Ion heating in the topside ionosphere has been investigated theoretically and also through numerical simulations by several authors [e.g., *Palmadesso et al.*, 1974; *Dusenbery and Lyons*, 1981; *Okuda and Ashour-Abdalla*, 1983]. We summarize here the results of a treatment appropriate to the conditions of Q machine experiments [*Dakin et al.*, 1976].

The time-averaged energy density, W, in an EIC wave can be written as [*Drummond and Rosenbluth*, 1962]

$$W = \frac{E_k^2}{8\pi}\left\{1 + \frac{1}{(k\lambda_{De})^2}\left[1 + \frac{T_i}{T_e\Gamma_n}\right]\right\} \tag{1}$$

with the usual meaning of the various symbols. The first term in braces is the electrostatic energy density of the wave, while the next two terms are the kinetic energy densities of the electrons and the ions, respectively. The kinetic energy density is much larger than the electrostatic energy density, since $(k\lambda_{De})^2 \ll 1$, while the ion kinetic energy density is larger than the electron kinetic energy density by a factor of $\approx\Gamma_n^{-1}$. If the wave field, E_k, is such that $E_k \sim \exp(\gamma t)$, then the rate of energy transfer to the ions, per unit volume, can be written as

$$\left(\frac{\partial U}{\partial t}\right)_{\text{ions}} = \frac{E_k^2}{4\pi}\frac{\gamma}{(k\lambda_{De})^2}\frac{T_i}{T_e\Gamma_1} \tag{2}$$

where only the fundamental ($n = 1$) wave mode is considered.

The energy gain given by (2) can be balanced against the main energy loss for the ions in the Q machine, which is a loss by convection to the end plates, namely,

$$\left(\frac{\partial U}{\partial t}\right)_{\text{ions}} \approx 2\kappa(T_i - T_0)\frac{n\langle v\rangle_i}{L} \tag{3}$$

where $\langle v\rangle_i$ is the ion convection velocity, L is the machine length, and T_0 is the end plate temperature. With [*Drummond and Rosenbluth*, 1962]

$$E_k = k\frac{\delta n}{n}\left(\frac{\kappa T_e}{e}\right)$$

and

$$\gamma = \left(\frac{\pi}{2}\right)^{1/2}\omega_{ci}\frac{T_e}{T_i}\Gamma_1\left(\frac{v_D}{v_e} - \frac{\omega_{ci}}{k_z v_e}\right)$$

where v_e is the electron thermal speed and v_D the relative electron-to-ion drift along **B**, one obtains

$$T_i^{1/2}(T_i - T_0) = 2.5\left(\frac{\pi m_i}{8\kappa}\right)^{1/2} LT_e\omega_{ci}\left(\frac{\delta n}{n}\right)^2\left(\frac{v_D}{v_e} - \frac{\omega_{ci}}{k_z v_e}\right) \quad (4)$$

Equation (4) (equation (12) of *Dakin et al.* [1976]) provides ion temperature enhancements, for $\delta n/n \sim 10$–20%, of up to factors of 10 over the normal Q machine ion temperatures, in general agreement with heating experiments.

A very simple, although rough, way of estimating the energization to be expected from the interaction of a typical Q machine ion with EIC waves is to assumed that the ion in question is phase locked with the wave **E** field, in such a way that it will gain an energy $(eE)\rho_i$ during the first half of its gyration period and another $(eE)\rho_i$ during the second half, when both the E field of the wave and the direction of the ion motion are reversed. Thus for the energy gain per gyroperiod, $\Delta\varepsilon$, we have $\Delta\varepsilon = 2eE\rho_i$. The power input into the ion can then be written as

$$P = \left(\frac{\omega_{ci}}{2\pi}\right)\Delta\varepsilon = 2ek\tilde{\phi}\rho_i\nu_{ci}$$

where $\nu_{ci} = \omega_{ci}/2\pi$ and $E = k\tilde{\phi}$. Since $e\tilde{\phi}/\kappa T_e = \delta n/n$, the rate of perpendicular energy increase is

$$\frac{d(E_\perp)}{dt} = P = 2(k\rho_i)(\kappa T_e)\nu_{ci}\left(\frac{\delta n}{n}\right) \approx 2(\kappa T_e)\nu_{ci}\left(\frac{\delta n}{n}\right) \quad (5)$$

when $k\rho_i \approx 1$. The energy gained by the ion during a traversal through the length l of the heating region, i.e., the axial region with appreciable $\delta n/n$, is then

$$\left(\frac{l}{v_{i,th}}\right)\frac{d(E_\perp)}{dt} = 2(\kappa T_e)\nu_{ci}\left(\frac{l}{v_{i,th}}\right)\left(\frac{\delta n}{n}\right) \quad (6)$$

With $\kappa T_e \simeq 0.2$ eV, $\delta n/n \simeq 0.2$, $l \simeq 15$ cm, $v_{i,th} \simeq 3 \times 10^4$ cm/s, and $\nu_{ci} \simeq 4 \times 10^4$ Hz, we find a total energy gain of ~ 1.6 eV. When the same type of argument is applied to ionospheric ions, with $\kappa T_e \approx 0.2$ eV, $v_{i,th} = 3 \times 10^5$ cm/s, $\nu_{ci} \approx 300$ Hz, and $\delta n/n \approx 0.05$, one finds energy gains of several keV, if the length of the heating region is of the order of ~ 1000 km.

2.2. *Energized Ions in a Diverging Magnetic Field*

Here we consider the evolution of the ion energies to be expected in a collisionless plasma in a diverging magnetic field. With reference to Figure 1, let the subscript zero refer to a region of relatively uniform magnetic field strength, in which ions are heated (e.g., by EIC waves) in a direction perpendicular to **B**. An ion of mass M with initial velocity components $(v_{\parallel,0}, v_{\perp,0})$ will flow along the diverging magnetic field lines under the action of the $-\boldsymbol{\mu}\cdot\nabla B$ force so that at some arbitrary axial location z is will have velocity components $(v_\parallel, v_\perp)$.

Let $B(z)$ be the magnetic field strength at a position z away from the heating region and define the mirror ratio $R(z) = B(z)/B_0$. In this analysis we will assume that the entire region from z_0 to z is at the same potential, although a small potential drop, of the order of 0.2 V, was present in our experiment along the diverging field lines. The effect of this potential drop will be discussed later (section 4.2). Conservation of the magnetic moment $\mu = (Mv_\perp^2/2B)$ and of the total energy, $(M/2)(v_\parallel^2 + v_\perp^2)$, requires that

$$v_\perp^2 = v_{\perp,0}^2\frac{B}{B_0} = v_{\perp,0}^2 R \quad (7)$$

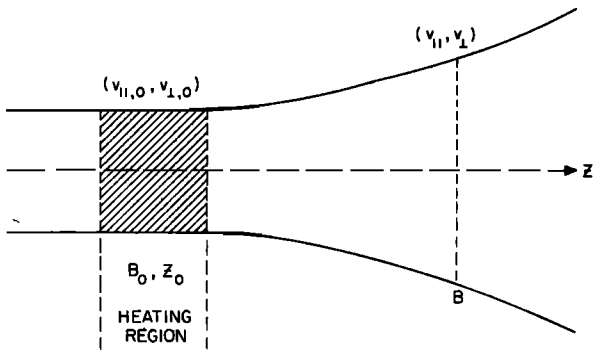

Fig. 1. Model for the calculation of ion energy distribution. Ions are heated in the perpendicular direction as they pass through the heating region and then flow out along the diverging **B** field lines, converting their perpendicular energy to parallel energy.

and

$$v_{\parallel,0}^2 + v_{\perp,0}^2 = v_\parallel^2 + v_\perp^2 \quad (8)$$

Substituting for $v_\perp^2$ from (7) into (8), we obtain

$$v_\parallel^2 = v_{\parallel,0}^2 + v_{\perp,0}^2(1 - R) \quad (9)$$

which expresses the transfer of energy from the perpendicular to the parallel direction as an ion moves toward the region of lower magnetic field strength. We may separate $v_\parallel$ into a "drift" component (the velocity of the ion "fluid" along **B**) and a "thermal" component, so that

$$v_\parallel = v_{\parallel,d} + v_{\parallel,t} \quad (10)$$

with the drift component being the same for all ions, while the thermal component accounts for the spread in $v_\parallel$ among the various ions. By squaring equation (10) and averaging over the ion velocity distribution, we find

$$\langle v_\parallel^2\rangle = v_{\parallel,d}^2 + \langle v_{\parallel,t}^2\rangle \quad (11)$$

since, by definition, $\langle v_{\parallel,t}\rangle = 0$. If now equation (9) is also averaged over the ion distribution and the result is combined with equation (11), one finds

$$\Delta E_d + \Delta(\kappa T_\parallel) = \kappa T_{\perp,0}(1 - R) \quad (12)$$

where

$$\Delta E_d = \tfrac{1}{2}M(v_{\parallel,d}^2 - v_{\parallel,0,d}^2)$$

$$\Delta(\kappa T_\parallel) = \tfrac{1}{2}M(\langle v_{\parallel,t}^2\rangle - \langle v_{\parallel,0,t}^2\rangle)$$

$$\kappa T_{\perp,0} = \tfrac{1}{2}M\langle v_{\perp,0}^2\rangle$$

Adding

$$\kappa T_\perp = \tfrac{1}{2}M\langle v_\perp^2\rangle = \kappa T_{\perp,0}R$$

to both sides of equation (12), we see further that

$$\Delta E_d + \Delta\kappa T_\parallel + \kappa T_\perp = \kappa T_{\perp,0} \quad (13)$$

which expresses the overall energy balance in terms of the measurable quantities. The predictions of this simple analysis based only on the conservation of magnetic moment and total energy will be compared with the experimental results in section 4.2. These simple considerations are in line with a more detailed theory developed by *Hatakeyama et al.* [1974], concerning the evolution of the ion distribution function in a nonuniform **B** field. They point out that as one moves from $z = z_0$ to larger values of z with R correspondingly decreasing,

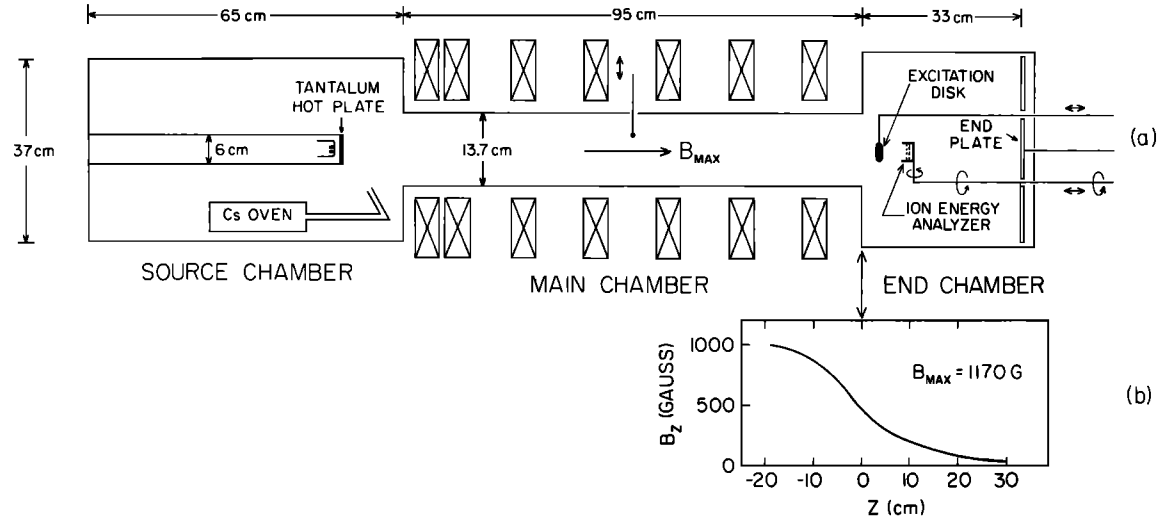

Fig. 2. The Iowa Q machine. (*a*) Schematic cross-sectional view. (*b*) Axial dependence of the **B** field in the end chamber.

the peak value of the parallel distribution function decreases, the distribution broadens, and the peak shifts toward a higher energy.

3. Experimental Setup

The experiments were performed in a single-ended Q machine shown schematically in Figure 2*a*. Cs plasma is produced by surface ionization of cesium atoms sprayed onto a hot (~2200°K) tantalum plate 6 cm in diameter and is confined radially by an axial magnetic field variable up to ~5 kG. The magnetic field is nonhomogeneous near the end of the device (Figure 2*b*), and its strength decreases rapidly with increasing z, as one moves into the end chamber, where the plasma is terminated by a large, cold, electrically floating end plate.

The chamber walls are cooled below 0°C to keep the neutral cesium vapor pressure below 10^{-6} torr. The plasma density, n, is typically of the order of 10^9 cm^{-3}, so that mean free paths for ion-ion and electron-ion collisions are of the order of 1 m. The neutral gas pressure is typically a few times 10^{-6} torr, corresponding to a mean free path for ion-neutral atom collisions of the order of several times the length of the device.

Electrostatic ion cyclotron waves are excited by biasing either a metallic disk (diameter 0.8 cm) or a metallic "ring" (outer diameter 0.8 cm, inner diameter 0.3 cm) at 1–2 V above the plasma potential, in order to draw an electron current along the axis of the device. Both the disk and the ring electrodes are movable along the axis. The ring electrode allows some measurements of the ion distribution, on axis, at various axial positions behind the exciter. Ion cyclotron waves are detected as electron current oscillations on the electrode or as ion current oscillations on various axially and radially movable disk Langmuir probes, 0.8 mm in diameter.

Ion energy distributions are obtained by means of a retarding potential analyzer, schematically shown in Figure 3*a*. Grid 1 is generally left floating, while the collector voltage is fixed at $V_c = -9$ V. The collector current, I_c, is recorded as a function of the retarding voltage, V_R, on grid 2. Typically, V_R is varied between -4 and $+4$ V. Figure 3*b* is an example of a recording obtained with the retarding potential analyzer, with the **B** field normal to the grid and collector planes. Such plots are digitized and then numerically differentiated to obtain dI_c/dV_R. The analyzer is movable both axially and radially, and at every position it can be rotated continuously relative to the direction of the **B** field.

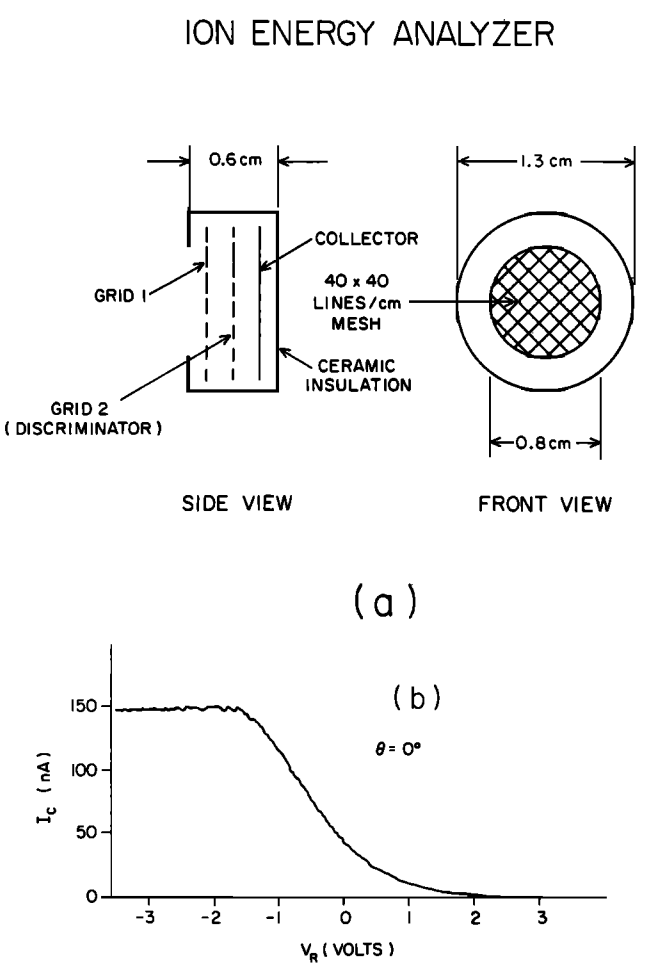

Fig. 3. (*a*) Schematic of the gridded, retarding potential analyzer used for ion energy measurements. (*b*) Typical characteristic of collector current, I_c, versus retarding grid voltage, V_R, with the ion energy analyzer normal along the **B** field.

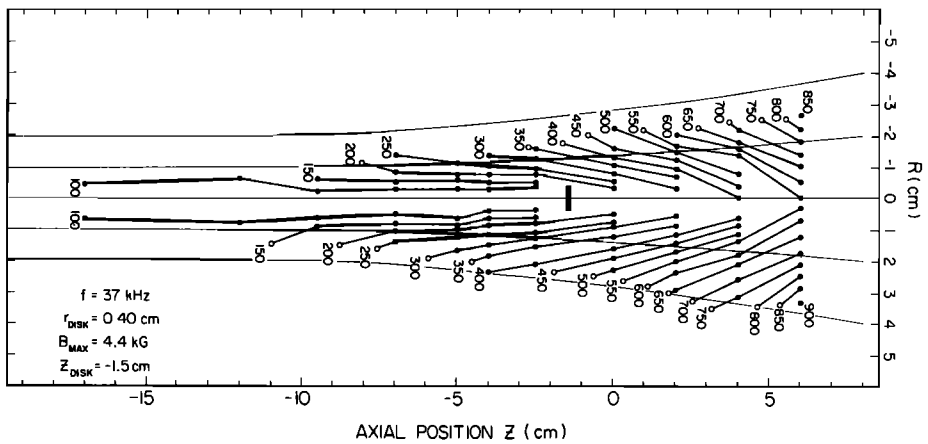

Fig. 4. EIC wave constant phase contours for an exciter ring located at $z = -1.5$ cm. The contours are labeled by a relative phase angle with wave propagation in the direction of increasing phase angle. A few **B** field lines are shown.

4. Experimental Results

4.1. *Data Presentation*

The EIC wave properties observed in the present magnetic field configuration have been described in detail in a previous paper [*Cartier et al.*, 1985*a*]. Figure 4, which is reproduced from that paper, shows constant phase contours for the EIC waves excited by drawing an electron current to a small disk. The wave fronts are labeled by their respective phase angles, with wave propagation in the sense of increasing phase angle and a change of phase by 360° equivalent to one wave period (for the case shown, $T = 27$ μs or $f = 37$ kHz). Ahead of the disk the waves propagate primarily radially outward from the current channel, although there is a clear, finite component of the propagation vector along **B**. The wave amplitude is large only within the current channel and varies from a $\delta n/n \simeq 1\%$ some 15 cm ahead of the disk to a $\delta n/n \approx 30\%$ close to the disk. The wave amplitude behind the disk is nowhere larger than a few percent. It seems clear that any heating of the plasma ions by EIC waves must predominantly take place in a small region just in front of the disk.

It is convenient to begin our presentation and discussion of the data on ion heating by showing in Figure 5*a* a set of data obtained with the ion energy analyzer located approximately 4.5 cm ahead of the exciter ring ($z \sim 7$ cm), just outside the current channel, and oriented with the opening parallel to the direction of the **B** field, as shown in the insert. In these semilog plots of the collector current, I_c, versus retarding voltage the slope of the line in the retarding region is a measurement of the ion temperature for a Maxwellian distribution. The four curves are for various biases on the exciter ring, $V_{ring} = -3.1$ V, -1.1 V, 0 V, and $+5.0$ V. EIC wave excitation is observed only for $V_{ring} \gtrsim -1.8$ V.

Figure 5*b* presents the same results of Figure 5*a* in differential form, dI_c/dV_R. These two ways of exhibiting the experimental data are essentially equivalent, but the differential form presentation is often convenient to deal with, since the ion energy distribution $f_i(E)$ is proportional to dI_c/dV_R (see, for example, *Andersen et al.* [1971] and *Stenzel et al.* [1982]). From the four plots of Figure 5*a* and additional data sets that are not shown, one infers that excitation of EIC waves of sufficiently large amplitude does indeed increase the perpendicular ion temperature from a $T_{i,\perp} \approx 0.15$–0.20 eV in the absence of waves to a $T_{i,\perp}$ as large as 1.5–2.0 eV when the disk is biased at $V_{ring} \gtrsim 10$ V. Figure 6 presents the measured $T_{i,\perp}$ as a function of V_{ring}, under the general conditions of Figure 5. Note that ion heating begins at $V_{ring} \gtrsim -1.8$ V, when wave excitation is first observed. One further point to notice, with reference to Figure 5*a*, is that at large V_{ring} one observes not only a general heating of the plasma ion population, sometimes referred to as "bulk" ions, but also the emergence of an even hotter population of "tail" ions. This phenomenon has been observed before in laboratory work on EIC waves [e.g., *Hatakeyama et al.*, 1977] and on numerical simulations of ion heating by the waves [e.g., *Okuda and Ashour-Abdalla*, 1983].

Next in our investigation we examined the ion energy distribution behind the exciter electrode where the magnetic field lines diverge, as a function both of the axial location of the energy analyzer and of the angle, θ, of the analyzer's normal direction relative to the magnetic field. An angle $\theta = 0°$ means that the analyzer "looks" into the ion flow along **B**, while at $\theta = 90°$ the analyzer "looks" transverse to **B**.

Figure 7 shows the differential analyzer curves, dI_c/dV_R, for $\theta = 0°$, at four axial positions behind an exciter ring electrode, i.e., at z equal to 3.6, 8.0, 13.7, and 26.4 cm. In this case the exciter ring (0.8 cm outside diameter; 0.3 cm inside diameter) was located at $z = -7.9$ cm and biased to excite EIC waves, while the analyzer was moved axially through the region of nonuniform magnetic field strength. As can be seen, the retarding voltage at which each curve attains its maximum, V_{max} (giving essentially the energy of maximum flux), increases continuously as the analyzer is moved to regions of weaker magnetic field. This increase of V_{max} with increasing z is not observed on the corresponding curves for $\theta = 90°$. Actually, for this data set, V_{max} for $\theta = 90°$ decreased slightly with increasing z; thus the increase in V_{max} seen in Figure 7 represents a real increase in directed energy.

This can also be seen in another set of measurements shown in Figure 8. The exciter ring position was in this case $z = 7.5$ cm. Analyzer plots were made for $\theta = 0°$ and $\theta = 90°$ at one axial position ahead of the ring just outside the current channel and three behind, all roughly along the same **B** field line. Again, V_{max} for $\theta = 0°$ increases with increasing z, as expected from the **B** field lines divergence. Accurate positioning of the analyzer is difficult, and the relatively large error bars reflect a radial dependence of V_{max}, arising because the effect of the EIC waves is largest on field lines which are nearest to the current channel. In addition, an apparent ion temperature,

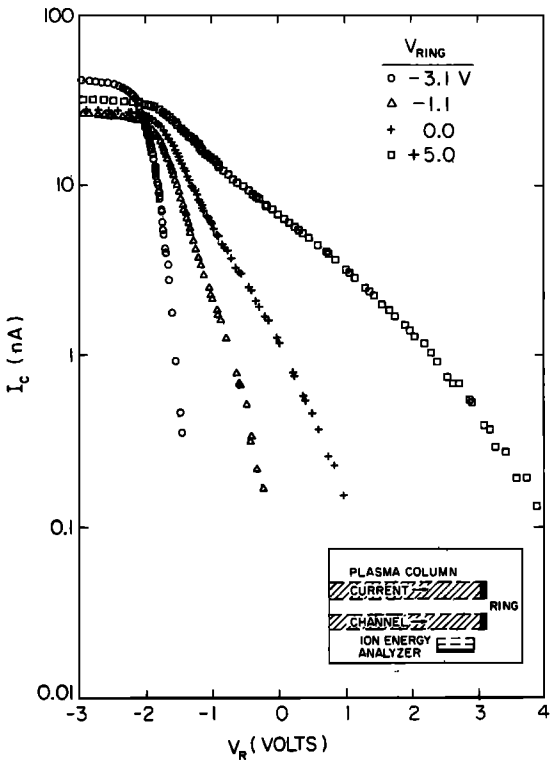

Fig. 5a

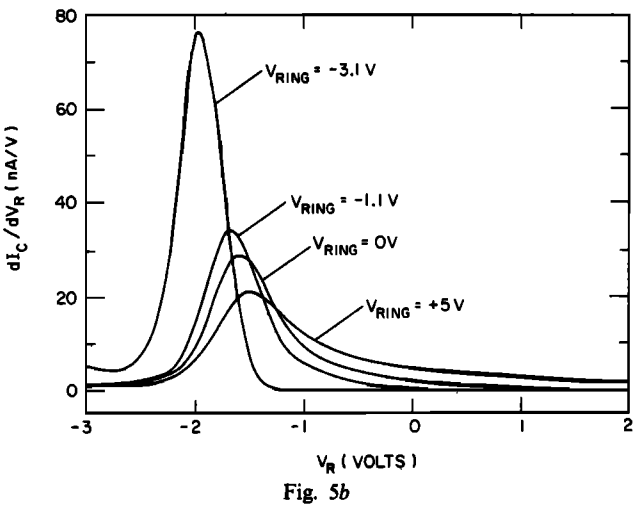

Fig. 5b

Fig. 5. Ion energy analyzer data for various exciter ring bias voltages. (*a*) Semilog plot of collector current I_c versus retarding voltage V_R. Insert shows analyzer location and orientation. (*b*) Differential form, dI_c/dV_R, of data presented in Figure 5*a*.

"T_i," as a function of both θ and axial position can be obtained from plots like that shown in Figure 5*a*. In Figure 9, "T_i (eV)" is shown for the same four axial positions of Figure 8 and $\theta = 0°$ and 90°. Evidently, with increasing z there is a continuous cooling in the perpendicular direction ($\theta = 90°$), accompanied by a continous heating in the parallel direction ($\theta = 0°$). The perpendicular cooling is from ~ 0.85 eV to ~ 0.4 eV, while the parallel heating is from ~ 0.25 eV to ~ 0.55 eV.

Additional data are shown in Figure 10 to further illustrate, by a somewhat different presentation, the general result of parallel energization as the ions move from high-**B** to low-**B** regions. This figure contains plots of the quantity V_{max}, defined

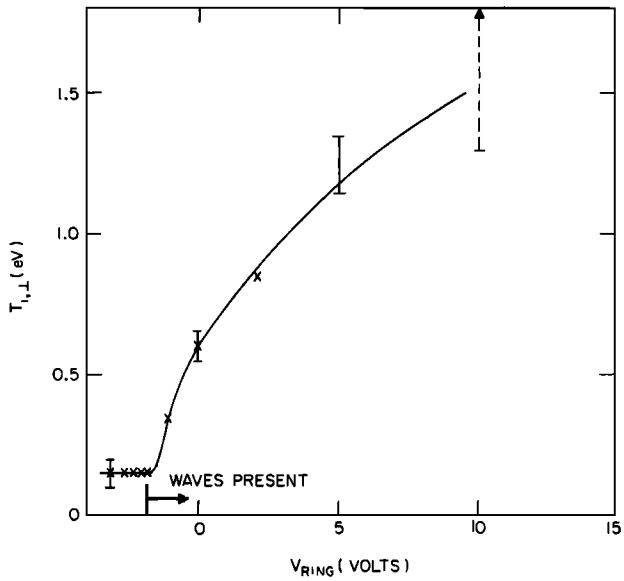

Fig. 6. Perpendicular ion temperature $T_{i,\perp}$ versus exciter ring bias measured in the heating region.

previously, versus the angle θ, for two values of z, $z_1 = 12.5$ cm and $z_2 = 25.1$ cm. For the case of Figure 10*a* the exciter ring was left electrically floating, so that no EIC waves were excited. The expected variation of V_{max} with θ is of the type $V_{max} = \text{const} + (\frac{1}{2}mv_d^2)\cos^2\theta$, where v_d is the net ion drift along **B** at the location of the measurements. Thus the variation of V_{max} between $\theta = 0°$ and $\theta = 90°$ should provide a measure of the ion parallel kinetic energy at the measurement location. Both plots, at z_1 and z_2, show the expected $\cos^2\theta$ variation and indicate an increase of the directed energy from ~ 0.5 eV to ~ 0.8 eV between z_1 and z_2. Figure 10*b* contains a similar plot, obtained at the same z_1 and z_2, when the exciter ring was biased at +3 V and EIC waves were excited. In this case the directed energy at z_1 is ~ 0.8 eV, while the directed energy at z_2 is ~ 1.3 eV.

In summary, the experimental results reported in this section show that (1) EIC waves heat the plasma ions perpendicularly to the **B** field, where increases in $T_{i,\perp}$ from ~ 0.2 eV to as much as ~ 2 eV are possible and (2) in a diverging **B** field geometry, energy is indeed transferred from perpendicular to

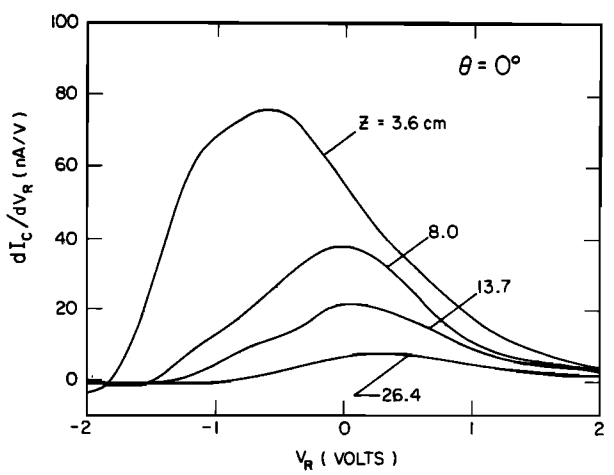

Fig. 7. Differential ion energy analyzer traces dI_c/dV_R with the analyzer looking along the magnetic field (into the ion flow) for various axial positions behind the exciter ring. The exciter ring is located at $z = -7.9$ cm.

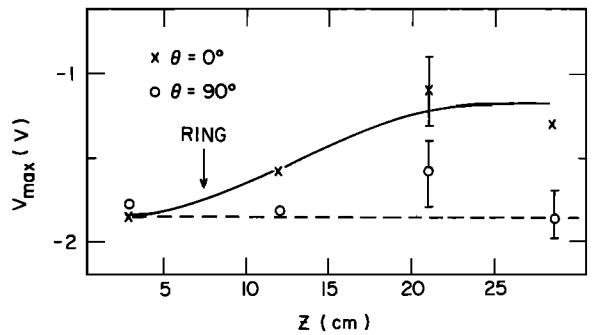

Fig. 8. V_{max}, voltage of maximum flux, versus z. The crosses correspond to $\theta = 0°$, and the circles correspond to $\theta = 90°$. Exciter ring is at $z = 7.5$ cm.

parallel motion, thus giving rise to an increase both in the parallel drift energy and in $T_{i,\parallel}$.

4.2. *Comparisons With Theory*

The experimental results presented in Figures 8 and 9 can be compared with the simple predictions of section 2.2. This comparison is shown in Figure 11, where the quantities $\kappa T_\perp$, ΔE_d, $\Delta\kappa T_\parallel$, and their sum are plotted versus R.

Figure 11*a* shows the decrease in the average perpendicular energy $\kappa T_\perp$ as the ions move in the region of weaker **B** field. The solid line is the prediction from the conservation of magnetic moment (equation (7)). Qualitatively, the trend of the data agrees with the prediction, although not as large a decrease in $\kappa T_\perp$ is observed. This may be possibly due to two factors. First, these measurements were made with the analyzer located slightly off axis with its normal oriented perpendicular to the axis. Off axis, where the analyzer is located, the diverging **B** field lines will not be exactly perpendicular to the analyzer opening so that the analyzer may also "see" a portion of the parallel flux. Second, any type of scattering processes that may occur (e.g., by collisions) would produce a larger $\kappa T_\perp$ than one would have in the absence of collisions.

The dependence of the increase in parallel drift energy, ΔE_d, and that of the thermal energy, $\Delta\kappa T_\parallel$, on R are shown in Figures 11*b* and 11*c*, respectively. The solid lines in both Figures 11*b* and 11*c* represent straight line fits to the equation $\Delta E_d = \alpha\kappa T_{\perp,0}(1 - R)$ and $\Delta\kappa T_\parallel = \beta\kappa T_{\perp,0}(1 - R)$. According to equation (12), the coefficients α and β should be such that $\alpha + \beta = 1$. Experimentally we find $\alpha + \beta \approx 1.1$.

The final plot of Figure 11 shows the sum of perpendicular ($\kappa T_\perp$) and parallel energies ($\Delta E_d + \Delta\kappa T_\parallel$), which, according to

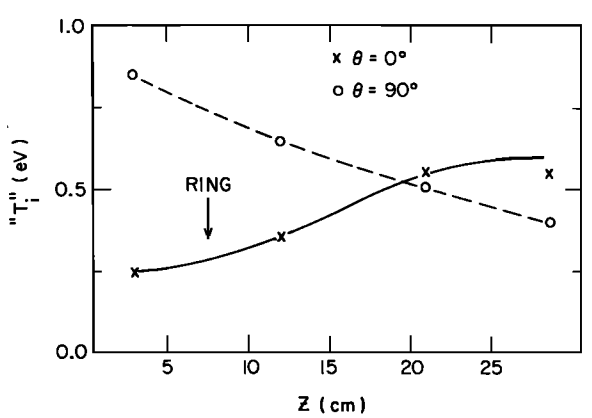

Fig. 9. Apparent ion temperatures for $\theta = 0$ (crosses) and $\theta = 90°$ (circles) versus z, for the same conditions as Figure 8.

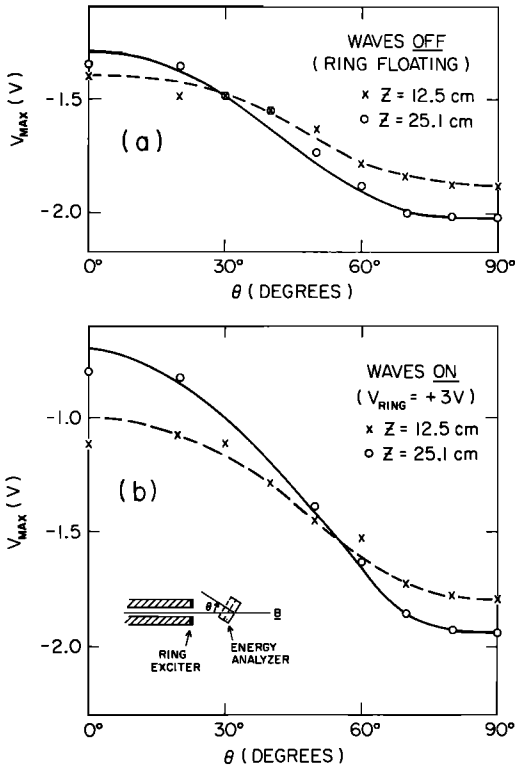

Fig. 10. Retarding voltage for maximum flux, V_{max}, versus θ, on axis and behind the exciter ring, at $z = 12.5$ cm (crosses) and $z = 25.1$ cm (circles). (*a*) EIC waves OFF, V_{ring} electrically floating. (*b*) EIC waves ON, $V_{ring} = +3$ V.

equation (13), should add up to the constant $\kappa T_{\perp,0}$. The data are in reasonable agreement with this prediction, although a small increase in total energy is apparent as the ions move into the weak **B** field region. This small increase may be accounted for by an additional energization mechanism, not included in the model of section 2.2, due to a small (0.2–0.3 V) potential drop which was measured along the magnetic field lines, moving from the high-**B** to the low-**B** region.

5. DISCUSSION AND CONCLUSIONS

Laboratory plasma experiments of space physics interest may generally be classified either as experiments of a "configuration simulation" type, aimed at simulating the actual configuration of a space system, or experiments of a "process simulation" type, in which the plasma physical process in question is studied in order to test available ideas or theories of space problems. In this paper we have presented results of an experiment of the "process simulation" type. The experimental results confirm the following:

1. EIC waves of sufficiently large amplitude are a powerful agent for transverse ion heating. The perpendicular ion temperature, $T_{i,\perp}$, is observed here to increase from $\sim$0.2 eV, in the absence of the waves, to as much as $\sim$2 eV when waves are present. This result is in general agreement with several previous laboratory experiments quoted earlier in the introduction.

2. Ions heated by the EIC waves in a region of high-**B** field transfer their energy from perpendicular to parallel motion as they pass through a region of diverging field lines. Both the parallel drift energy and the parallel thermal energy are observed to increase, at the expense of the initial perpendicular energy.

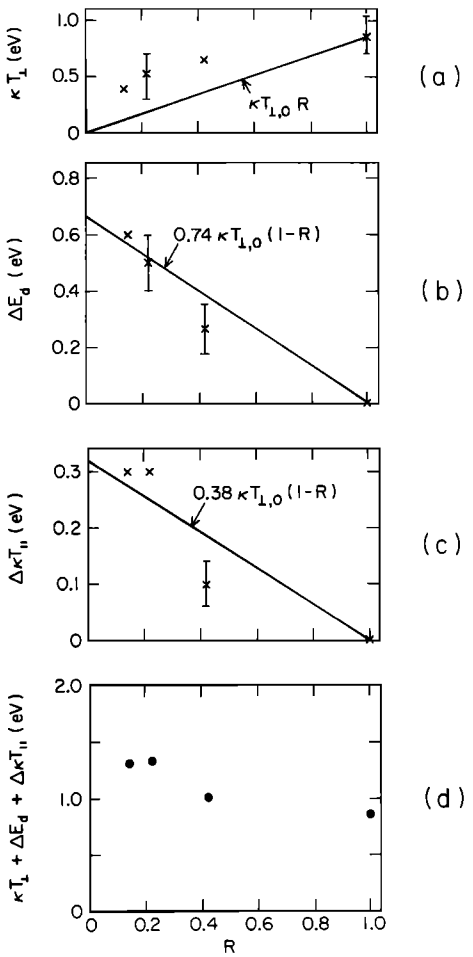

Fig. 11. Comparisons with theory. (*a*) $\kappa T_\perp$ values versus R, the mirror ratio $[B(z)/B_0]$. (*b*) ΔE_d versus R. (*c*) $\Delta\kappa T_\parallel$ versus R. (*d*) The sum $\kappa T_\perp + \Delta E_d + \Delta\kappa T_\parallel$ versus R.

In attempting to relate these results to the ionosphere-magnetosphere system it is essential to point out certain important differences between the laboratory and space configurations. In particular, the Q machine plasma is bounded with peculiar end conditions which are not directly applicable to the essentially infinite plasma of the ionsophere-magnetosphere system. Specifically, the ion distribution function in this experiment is one-sided, and there are essentially no phase space points in the negative $v_\parallel$ half plane. Under such conditions a flowing plasma is produced in the reduced magnetic field region. In the space environment such boundaries do not exist, and the distribution function in the "heating region" is fully developed (i.e., both positive and negative $v_\parallel$ are represented).

Also, the detector used in this experiment has a very broad angular response, whereas the instruments used in the space measurements have much narrower viewing angles, so that one measures $f(v_\parallel, v_\perp)$ at many different points in $(v_\parallel, v_\perp)$ space (see, for example, *Mizera and Fennell* [1977]). In our retarding potential analyzer, when θ is zero (see Figure 10*b*), the instrument is essentially performing an integral over the distribution function over all $v_\perp$. Thus the distribution function which we measured here is essentially

$$F(v_\parallel) = 2\pi \int f(v_\parallel, v_\perp) v_\perp \, dv_\perp$$

as distinct from $f(v_\parallel, v_\perp = 0)$.

With these important differences in mind it seems reasonable to conclude that the main results summarized above in points 1 and 2 may be relevant for the process of ion conic formation as discussed, e.g., by *Klumpar* [1975, 1979], *Kintner et al.* [1978], and *Ungstrup et al.* [1979]. In comparing the laboratory results with the space measurements we stress again that one should be careful in scaling the parameters up to the actual space configuration. For example, the temperature gains observed in the laboratory are considerably smaller than the heating gains inferred from the conic measurements in space. This is primarily due to the fact that although EIC wave amplitudes approaching 30% are present in front of the laboratory exciter electrodes, the heating is confined to a relatively small axial region. In the ionospheric case, on the other hand, the heating region may extend over several thousands of kilometers with EIC wave amplitudes of 2–5%.

Whether or not other processes, such as the acceleration associated with oblique double layers [*Lennartsson*, 1980; *Borovsky*, 1981; *Borovsky and Joyce*, 1983] or the energization by lower hybrid waves [*Chang and Coppi*, 1981], may also be important in the formation of conics in the earth's magnetosphere, or even be more important than the mechanism we have investigated, cannot be decided by our experiment. The answer to this question must be left to in situ observations.

Acknowledgments. We wish to thank Al Scheller for his help in the construction and maintenance of the Iowa Q machine. This work was supported by the U.S. Office of Naval Research and in part by NASA grant NGL 16-001-043 and by a Northwest Area Foundation grant of the Research Corporation.

The Editor thanks D. M. Klumpar and N. Rynn for their assistance in evaluating this paper.

REFERENCES

Alport, M. J., P. J. Barrett, and M. A. Behrens, Selective destabilization of ion cyclotron modes, *Plasma Phys., 25*, 1059, 1983.

Andersen, S. A., V. O. Jensen, P. Michelsen, and P. Nielsen, Determination and shaping of the ion-velocity distribution function in a single-ended Q machine, *Phys. Fluids, 14*, 728, 1971.

Bakshi, P., G. Ganguli, and P. L. Palmadesso, Finite-width currents, magnetic shear, and the current-driven ion-cyclotron instability, *Phys. Fluids, 26*, 1808, 1983.

Bergmann, R., Electrostatic ion (hydrogen) cyclotron and ion acoustic wave instabilities in regions of upward field-aligned current and upward ion beams, *J. Geophys. Res., 89*, 953, 1984.

Borovsky, J. E., The simulation of plasma double layer structures in two dimensions, Ph.D. thesis, University of Iowa, Iowa City, 1981.

Borovsky, J. E., The production of ion conics by oblique double layers, *J. Geophys. Res., 89*, 2251, 1984.

Borovsky, J. E., and G. Joyce, Numerically simulated two-dimensional auroral double layers, *J. Geophys. Res., 88*, 3116, 1983.

Cartier, S. L., N. D'Angelo, and R. L. Merlino, Electrostatic ion-cyclotron waves in a nonuniform magnetic field, *Phys. Fluids, 28*, 3066, 1985*a*.

Cartier, S. L., N. D'Angelo, P. H. Krumm, and R. L. Merlino, Filamental quenching of the current-driven ion-cyclotron instability, *Phys. Fluids, 28*, 432, 1985*b*.

Chang, T., and B. Coppi, Lower hybrid acceleration and ion evolution in the supra-auroral region, *Geophys. Res. Lett., 8*, 1253, 1981.

Chu, T. K., S. Bernabei, and R. W. Motley, Parametrically driven ion cyclotron waves and intense heating, *Phys. Rev. Lett., 31*, 211, 1973.

Correll, D. L., N. Rynn, and H. Bohmer, Onset, growth, and saturation of the current-driven ion cyclotron instability, *Phys. Fluids, 18*, 1800, 1975.

Correll, D. L., H. Bohmer, N. Rynn, and R. A. Stern, Temporal evolution of ion temperatures in the presence of ion cyclotron instabilities, *Phys. Fluids, 20*, 822, 1977.

Croley, D. R., Jr., P. F. Mizera, and J. F. Fennell, Signature of a parallel electric field in ion and electron distributions in velocity space, *J. Geophys. Res., 83*, 2701, 1978.

Dakin, D. R., T. Tajima, G. Benford, and N. Rynn, Ion heating by the electrostatic ion cyclotron instability: Theory and experiment, *J. Plasma Phys.*, *15*, 175, 1976.

D'Angelo, N., and R. W. Motley, Electrostatic oscillations near the ion cyclotron frequency, *Phys. Fluids*, *5*, 663, 1962.

Drummond, W. E., and M. N. Rosenbluth, Anomalous diffusion arising from microinstabilities in a plasma, *Phys. Fluids*, *5*, 1507, 1962.

Dusenbery, P. B., and L. R. Lyons, Generation of ion conic distribution by upgoing ionospheric electrons, *J. Geophys. Res.*, *86*, 7627, 1981.

Frank, L. A., K. L. Ackerson, and D. M. Yeager, Observations of atomic oxygen (O^+) in the earth's magnetotail, *J. Geophys. Res.*, *82*, 129, 1977.

Ganguli, G., and P. Bakshi, Nonlocal aspects of electrostatic current-driven ion cyclotron instability due to magnetic shear, *Phys. Fluids*, *25*, 1830, 1982.

Ganguli, G., P. Bakshi, and P. Palmadesso, Electrostatic ion-cyclotron waves in magnetospheric plasmas: Nonlocal aspects, *J. Geophys. Res.*, *89*, 945, 1984.

Ghielmetti, A. G., R. G. Johnson, R. D. Sharp, and E. G. Shelley, The latitudinal, diurnal and altitudinal distributions of upward flowing energetic ions of ionospheric origin, *Geophys. Res. Lett.*, *5*, 59, 1978.

Hatakeyama, R., N. Sato, Y. Tsunoda, H. Sugai, and Y. Hatta, Ion-energy distribution in a plasma under a diverging magnetic field, *J. Appl. Phys.*, *45*, 85, 1974.

Hatakeyama, R., N. Sato, H. Sugai, and Y. Hatta, Enhanced heating of mirror trapped ions under an instability around ion-cyclotron frequency, *Phys. Lett.*, *63A*, 28, 1977.

Horwitz, J. L., The ionosphere as a source for magnetospheric ions, *Rev. Geophys.*, *20*, 929, 1982.

Kintner, P. M., M. C. Kelley, and F. S. Mozer, Electrostatic hydrogen cyclotron waves near one earth radius altitude in the polar magnetosphere, *Geophys. Res. Lett.*, *5*, 139, 1978.

Kintner, P. M., M. C. Kelley, R. D. Sharp, A. G. Ghielmetti, M. Temerin, C. Cattell, P. F. Mizera, and J. F. Fennell, Simultaneous observations of energetic (keV) upstreaming and electrostatic hydrogen cyclotron waves, *J. Geophys. Res.*, *84*, 7201, 1979.

Klumpar, D. M., Evidence for ion acceleration by VLF waves above the auroral ionosphere, paper presented at the Canadian Association of Physicists Congress, Toronto, June 1975.

Klumpar, D. M., Transversely accelerated ions: An ionospheric source of hot magnetospheric ions, *J. Geophys. Res.*, *84*, 4229, 1979.

Lang, A., and H. Boehmer, Electron current disruption and parallel electric fields associated with electrostatic ion cyclotron waves, *J. Geophys. Res.*, *88*, 5564, 1983.

Lennartsson, W., On the consequences of the interaction between the auroral plasma and the geomagnetic field, *Planet. Space Sci.*, *28*, 135, 1980.

Levine, A. M., and A. F. Kuckes, Excitation of electrostatic ion cyclotron oscillations, *Phys. Fluids*, *9*, 2263, 1966.

Michelsen, P., H. L. Pécseli, J. Juul Rasmussen, and N. Sato, Unstable electrostatic ion cyclotron waves excited by an ion beam, *Phys. Fluids*, *19*, 453, 1976.

Mizera, P. F., and J. F. Fennell, Signatures of electric fields from high and low altitude particle distributions, *Geophys. Res. Lett.*, *4*, 311, 1977.

Motley, R. W., and N. D'Angelo, Excitation of electrostatic plasma oscillations near the ion cyclotron frequency, *Phys. Fluids*, *6*, 296, 1963.

Okuda, H., and M. Ashour-Abdalla, Acceleration of hydrogen ions and conic formation along auroral field lines, *J. Geophys. Res.*, *88*, 899, 1983.

Okuda, H., and K. I. Nishikawa, Ion-beam-driven electrostatic hydrogen cyclotron waves on auroral field lines, *J. Geophys. Res.*, *89*, 1023, 1984.

Palmadesso, P. J., T. P. Coffey, S. L. Ossakow, and K. Papadopoulos, Topside ionosphere ion heating due to electrostatic ion cyclotron turbulence, *Geophys. Res. Lett.*, *1*, 105, 1974.

Sato, N., and R. Hatakeyama, A mechanism for potential-driven electrostatic ion cyclotron oscillations in a plasma, *J. Phys. Soc. Jpn.*, *54*, 1661, 1985.

Schrittwieser, R., N. Rynn, R. Koslover, and R. Karim, Can the electrostatic ion-cyclotron instability be driven by a two-dimensional sheath?, *Plasma Phys. Controlled Fusion*, *26*, 1591, 1984*a*.

Schrittwieser, R., N. Rynn, R. Koslover, and R. Karim, Electrostatic ion-cyclotron instability driven by a slow electron drift, *Plasma Phys. Controlled Fusion*, *26*, 1597, 1984*b*.

Sharp, R. D., R. G. Johnson, and E. G. Shelley, Observation of ionospheric acceleration mechanism producing energetic (keV) ions primarily normal to the geomagnetic field direction, *J. Geophys. Res.*, *82*, 3324, 1977.

Shelley, E. G., R. D. Sharp, and R. G. Johnson, Satellite observations of an ionospheric acceleration mechanism, *Geophys. Res. Lett.*, *3*, 654, 1976.

Stenzel, R. L., R. Williams, R. Aguero, K. Kitazaki, A. Ling, T. McDonald, and J. Spitzer, Novel directional ion energy analyzer, *Rev. Sci. Instrum.*, *53*, 1027, 1982.

Stern, R. A., D. L. Correll, H. Bohmer, and N. Rynn, Nonlocal effects in the electrostatic ion-cyclotron instability, *Phys. Rev. Lett.*, *37*, 833, 1976.

Stern, R. A., D. N. Hill, and N. Rynn, Azimuthal coherent ion-ring-beam generation in an unstable magnetized plasma, *Phys. Rev. Lett.*, *47*, 792, 1981.

Ungstrup, E., D. M. Klumpar, and W. J. Heikkila, Heating of ions to superthermal energies in the topside ionosphere by electrostatic ion cyclotron waves, *J. Geophys. Res.*, *84*, 4289, 1979.

Varma, R. K., and D. Bhadra, Collisional effects in a hot plasma at ion gyrofrequency, *Phys. Fluids*, *7*, 1082, 1964.

S. L. Cartier, N. D'Angelo, and R. L. Merlino, Department of Physics and Astronomy, University of Iowa, Iowa City, IA 52242.

(Received October 18, 1985;
revised January 24, 1986;
accepted March 3, 1986.)